



N-Decane Reforming by Gliding Arc Plasma in Air and Nitrogen

Feilong Song¹ · Yun Wu^{1,2} · Shida Xu¹ · Xingkui Yang¹ · Yuanbo Xuan³

Received: 2 June 2020 / Accepted: 27 July 2020 / Published online: 16 August 2020
© Springer Science+Business Media, LLC, part of Springer Nature 2020

Abstract

Plasma cracking of n-decane is carried out in a new type of gliding arc flow reactor in the atmosphere of nitrogen and air, at a flow range of 25–45 L/min with an interval of 5 L/min. The relationship between arc evolution and discharge voltage and current signals is established by synchronous recording with high-speed camera and oscilloscope. It is recorded that the rotating frequency of the gliding arc is in the range of 81–176 Hz, which increases with the rise of the flow rate and has no direct relationship with the type of gas. When air is used as the discharge medium, although the luminous intensity of the arc is weak, arc rotation is relatively stable, and the specific input energy is higher, which is 58% higher than that of nitrogen. In addition, the partial oxidation of n-decane provides extra heat for cracking, which is helpful to improve the efficiency of plasma cracking. The cracking products mainly include hydrogen, ethylene, acetylene, methane, propylene and ethane. The concentration of each component is higher, reaching the maximum value at the flow rate of 40 L/min, with the hydrogen selectivity of 23.1%. However, when nitrogen plasma is selected, the kinds of products are reduced, containing only hydrogen, ethylene and acetylene, and the concentrations are lower than 0.5%. Two parameters, energy conversion efficiency and carbon based characterization effective cracking rate, were proposed to evaluate the cracking effect of flow reactor.

Keywords N-decane · Cracking · Gliding arc plasma · Selectivity

Introduction

The traditional rotating detonation combustor (RDC) is an annular combustor. The detonation wave propagates along the circumferential direction and the combustion products are discharged in the axial direction. Compared with the traditional Brayton cycle,

✉ Yun Wu
wuyun1223@126.com

¹ Science and Technology on Plasma Dynamics Laboratory, Air Force Engineering University, Xi'an 710038, China

² Institute of Aeroengine, School of Mechanical Engineering, Xi'an Jiaotong University, Xi'an 710049, China

³ Aeronautics Engineering College, Air Force Engineering University, Xi'an 710038, China

the detonation combustion cycle has higher combustion efficiency [1], higher propulsion performance [2], and has the advantage of compact structure [3]. Compared with the traditional turbine engine combustion chamber structure, the annular combustion chamber structure is simpler [4], making it more suitable for use in existing aviation jet turbine engines. In terms of propulsion performance, the specific fuel consumption rate in RDC is about 30% lower than that of a traditional afterburner, while the unit thrust is at least 30% higher than that of a traditional afterburner [5].

At present, the research on rotating detonation mainly focuses on gas fuels such as hydrogen [6] and ethylene [7]. However, the liquid fuels must be used for aviation engines. Since aviation fuel cannot be affected by extreme temperatures, especially below freezing point, it is also required that the fuel has a higher flash point to make it less flammable, thus ensuring a lower risk of handling and transportation. Therefore, most aviation fuels are still kerosene-based [8]. Due to the low activity of kerosene, it is difficult to directly use liquid kerosene and pure air as propellants for rotating detonation experiments, usually adopting hydrogen doping [9], supplementing oxygen [10], pre-evaporation [11] or heating air [12] as an auxiliary means. From the analysis of the research results, these methods are conducive to the realization of kerosene detonation combustion. However, the maintenance of detonation combustion requires the addition of highly active gases such as hydrogen and oxygen. The limited availability of highly active gases limits working hours and the absence of heat sources during startup, making the above approach unsuitable for aeroengine applications. Therefore, there is an urgent need to find innovative ways suitable for application to assist kerosene initiation.

Austin's detonation initiation experiment with cracking product of JP-10 kerosene in 2002 [13] proved that the active small molecule gas generated by cracking can greatly reduce the difficulty of kerosene initiation [14]. Using cracking technology to crack kerosene to generate small molecular gaseous species, including hydrogen, ethylene, acetylene and other components that are prone to detonation, is expected to solve the problem of kerosene detonation. Compared with traditional catalytic cracking and thermal cracking, plasma is a clean and efficient energy source with high activity and no problem of catalyst failure [15]. It has obvious advantages in the treatment of hydrocarbon fuel. It is widely used in the reforming of small-molecular hydrocarbons to obtain hydrogen-rich gas [16, 17], oil modification, etc. [18, 19]. In view of the fuel cracking characteristics of different fuels, different discharge structures, and discharge forms of plasma, many research institutions have carried out a lot of valuable research. Among them, Rueangjitt et al. [20] studied the effects of methane concentration, air intake rate, discharge interval, residence time and catalytic distance on methane non-oxidative cracking reforming by gliding arc plasma. The study found that acetylene and hydrogen are mainly produced with high selectivities of about 70–90% and 75%, and the closer the catalyst distance, the higher the methane conversion rate. Jiang et al. [21] innovatively proposed a three-electrode gliding arc flow reactor, which successfully achieved the improvement of toluene emission reduction. The study found that in terms of toluene degradation and energy yield, a shorter gap between electrodes and a longer discharge length are more advantageous. Sreethawong et al. [22] used multi-stage gliding arc to partially oxidize methane to produce syngas. The results show that, contrary to the increase of CH_4/O_2 molar ratio, the effect of feed flow rate and frequency is opposite, increasing the number of gliding arc stages, voltage, or electrode gap distance can simultaneously increase CH_4 and O_2 conversion. Rollier et al. [23, 24] have conducted a long-term study on the application of plasma to hydrocarbon fuel conversion. Two types of fuel cracking reformers based on gliding arc plasma have been successfully used to achieve the cracking of on-board gasoline. Taghvaei et al. [25] studied the

characteristics of nanosecond pulsed dielectric barrier discharge through experiments, and clarified the effect of hydrocarbon chain length and carrier gas type (Ar, Ar-CH₄ mixed gas) on plasma cracking to produce hydrogen. The influence of hydrocarbon chain length was investigated using C₁-C₁₆ straight-chain alkanes. The results show that due to the increase in the carbon number of the feedstock hydrocarbon, the reactor performance is significantly improved.

In summary, for various backgrounds, plasma cracking has been widely applied, but the design and research work of the reactor combined with aviation kerosene is still blank. Our research group has carried out various forms of DBD plasma for fuel cracking research using n-decane, a single alternative fuel for aviation kerosene, and is committed to optimizing the structure of the flow reactor, improving the cracking efficiency, and regulating the distribution of cracking gas components [26–29]. This paper further proposes a plasma flow reactor with rotating gliding arc for cracking and reforming n-decane under higher fuel flow rate in order to obtain more active gas and improve the performance of the rotating detonation combustor.

Experimental Approach

The experimental system is shown in Fig. 1. The experiments were conducted in air and nitrogen environments, and the gas supply system was opened to clean the pipelines and reactors before the experiment. The gas flow is controlled by a pressure gauge and a ball valve, of which the rate is monitored by a turbine flow meter (D08-1, range 0–200 L/min, accuracy 2%) to ensure that a stable flow enters the experimental device. Liquid n-decane is stored in the fuel tank. The nitrogen high-pressure bottle and pressure reducing valve ensure that the fuel supply pressure is 0.7 MPa to realize fuel flow rate is

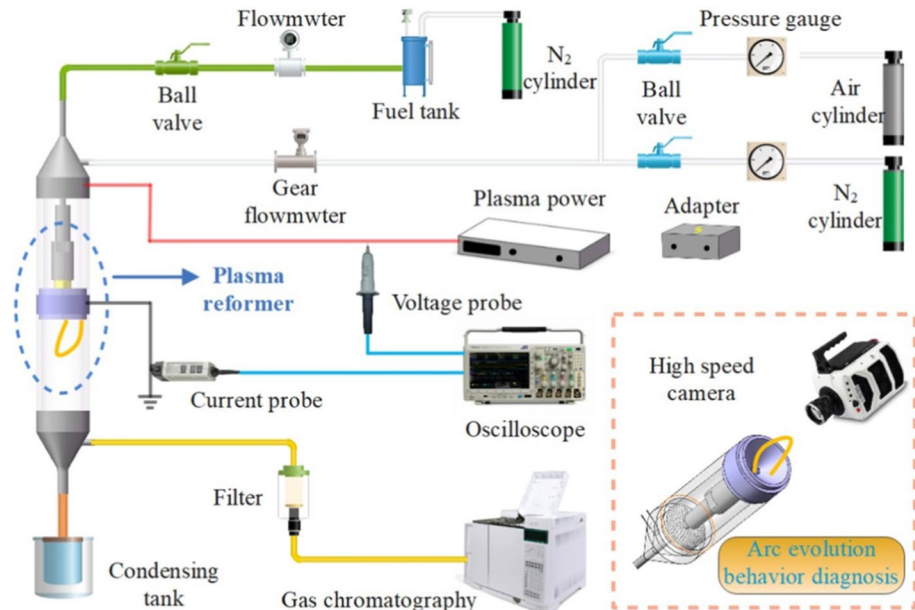


Fig. 1 Schematic of experimental setup for cracking n-decane by gliding arc plasma

always maintained at 22 mL/min, which is measured by a gear flow meter (CX-M2, range 0.5–150 mL/min, accuracy 0.5%). This experiment uses millisecond AC power supply (CTP-2000 K) for power supply, the peak output voltage range is 30 kV, and the excitation frequency range is 6–30 kHz. The high voltage output of the power supply is connected to the fuel injector located on the central axis in the experimental device, and the venturi nozzle is grounded to realize the arc discharge between the fuel injector and the venturi nozzle. The discharge parameters are measured with high voltage probe (P6015A) and current probe (TCP0030A). Data acquisition uses digital oscilloscope (MDO3024). Use the phantomv2512 high speed camera to capture the details of the discharge. The maximum shooting speed is 20,000 frames per second under the resolution of 1024*1024, while the minimum resolution is used, the maximum shooting speed is 670,000 frames per second. The parameters used in this article are a resolution of 512*384, a shooting frequency of 40,000 frames, and an exposure time of 23.6 μ s.

Plasma cracking products are detected on-line using a gas chromatograph (Agilent 7890B). The gas chromatograph is equipped with two thermal conductivity detectors (TCD) and one flame ionization detector (FID). One TCD is used to analyze hydrogen, and the other TCD is used to analyze carbon dioxide, carbon monoxide, oxygen, and nitrogen. FID can quantitatively analyze the following substances: alkanes, alkenes and alkynes with three carbon atoms or less; alkanes and alkenes with four carbon atoms; n-pentane and isopentane. The detection threshold of TCD is about 200 ppm, and FID is 2 ppm. Each experimental condition was repeated sampling and analysis three times to obtain concentration data with an error of less than 3%. The data used in this article is the average of the three results.

The structure of the reactor is shown in Fig. 2. The outer cylinder of the reactor is composed of three parts: the upper end is the fuel and gas inlet section, which is made of stainless steel; two plexiglass tubes of equal length are used as the outer shell to observe the experimental state, of which the length is 100 mm, the outer diameter is 50 mm, and the thickness is 2.5 mm; the lower end is the outlet part of cracking product and waste liquid. The cracking product enters the chromatography through the filter by the downstream

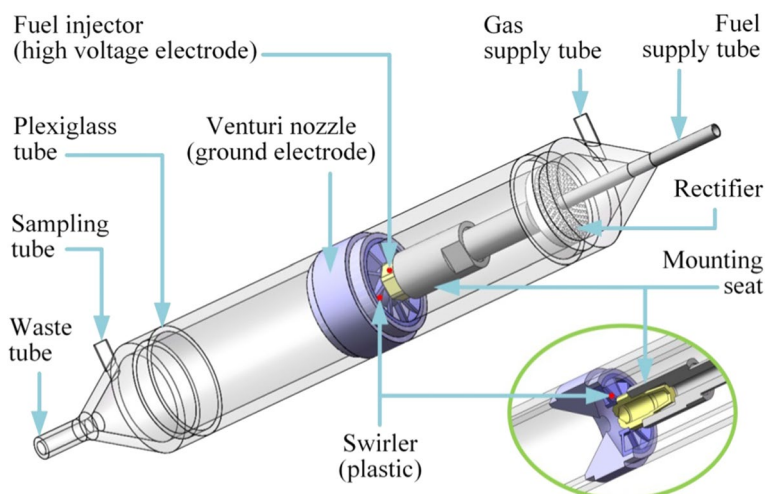


Fig. 2 Scheme of the plasma reactor

sampling tube. The waste liquid generated by plasma cracking enters the condensate tank by the waste tube to prevent contamination of the chromatography or block the pipeline. After the gas enters the reactor through the pipeline, a stable and uniform gas flow is generated through the upstream rectifier and enters the downstream channel by the swirler. The swirler is a 3D printed plastic product to ensure the insulation between the high pressure electrode and the ground electrode. The swirler is located 90 mm downstream of the rectifier, of which the outer diameter is 36 mm, the number of blades is 10, the angle of the swirl blades is 45°, and the number of swirls is 0.78. The fuel enters the reactor by the supply pipe. And then it is sprayed into the plasma cracking reaction zone by the atomizing injector (Danfoss). The venturi nozzle is in the form of an expansion nozzle, with a diameter of 8 mm at the minimum cross section and an axial distance of 7 mm from the fuel injector to achieve arc discharge between the fuel injector and the venturi nozzle.

The input power of millisecond AC power to the cracker is calculated by formula (1):

$$P = \int_0^t U \cdot I / t \tag{1}$$

In the formula: U and I are the corresponding voltage value and current value within the integration time respectively, of which the unit is V and A.

Specific input energy (SIE) is defined as:

$$SIE = \frac{60P}{q_v} \tag{2}$$

In the formula: the unit of SIE is J/L ; q_v is gas volume flow rate, unit is L/min .

The selectivity, energy conversion efficiency and effective cracking rate are used to evaluate the distribution of cracking products and the effects of cracking, which are defined as follows:

$$H_2 \text{ selectivity}(\%) = \frac{\text{Amount of H atoms in the formed } H_2}{\text{Total amount of H atoms in the products}} \times 100\% \tag{3}$$

The products involved in formula (3) include the main cracking products detected by gas chromatograph, and the products with concentration level of 1/10,000 are ignored.

$$\text{Energy conversion efficiency} = \frac{\sum_i m_i \times LHV_i}{m_f \times LHV_f} \tag{4}$$

In formula (4), m_i is the mass flow rate of each cracking product, LHV_i is the low heating value of the corresponding component, m_f is the mass flow rate of n-decane, and LHV_f is the low heating value of n-decane.

$$\text{Effective cracking rate}_{\text{based on carbon atom}} = \frac{\sum_i \frac{P_{C_xH_y \text{ or } CO_2} \times \frac{F_{N_2}}{P_{N_2}}}{V_m} \times N_{C_xH_y \text{ or } CO_2} \times M_C}{m_c} \tag{5}$$

In formula (5), F and P represent volume flow rate (L/s) and volume percentage (%); M_c is the molar mass of carbon (g/mol); N is the number of carbon atoms in the molecular formula of C_xH_y or CO_2 ; V_m is the gas molar volume (L/mol); m_c is the mass flow rate of carbon in n-decane (g/s). The oxygen-containing products formed when discharged in the

air have not been measured. Therefore, the values calculated by (3) are overestimated, and the values calculated by (4) and (5) are underestimated.

Results and Discussion

Characteristics Analysis of Gliding Arc Discharge

A high-speed camera is used to capture the gliding arc formed between the fuel injector and the venturi. At this time, the downstream plexiglass tube, sampling tube and other components are removed, and the fuel supply is stopped, just providing an air flow of 25 L/min to form a swirling airflow through the swirler. The high speed camera axially faces the discharge area, and the lens focuses on the fuel injector. As shown in Fig. 3, the gliding arc rotating area is mainly within the blue dotted frame. The gliding arc discharge is a thin, arc-shaped plasma column sweeping along the circumference of the venturi nozzle. The gliding arc plasma column has three stages in a discharge process: the breakdown between the fuel injector and the venturi nozzle, the elongation of the arc and the extinction. It should be noted that the extinction of the arc does not refer to the complete quenching of the arc, but rather that a short circuit occurs on the plasma column when stretched long enough and the arc generates wrinkles, causing the arc length to be shortened instantly.

In the initial stage of discharge, set the voltage value through the trigger function of the oscilloscope. When the loading voltage between the venturi nozzle and the fuel injector reaches the set value, the oscilloscope sends a trigger signal to the high speed camera to record the image of the arc discharge process. At the same time, the oscilloscope simultaneously records the voltage and current signals of the gliding arc discharge, as shown in Fig. 4. After the power was turned on in the experiment, the voltage signal instantaneously rose to the maximum voltage value, about 15 kV, and the current increased more than 8 A, which provided the required electric field for the initial breakdown of the gliding arc, and this time was recorded as t_0 . The subsequent discharge reached a relatively stable stage, and the envelope voltage showed periodic oscillations within 7 kV, lasting about 1 ms. The plasma column from t_0 to t_1 in Fig. 3 shows a typical stable gliding arc with a smooth arc-shaped discharge channel. The arc gradually elongates while rotating circumferentially under the action of the gas flow. The current at this stage is glow discharge [30], the voltage waveform is a sine wave, and the current is less than 1 A. With the extension of the gliding arc, the voltage required to maintain the arc gradually increased. At t_1 , the peak voltage suddenly increased, and the corresponding current exceeded 2 A, becoming a spark

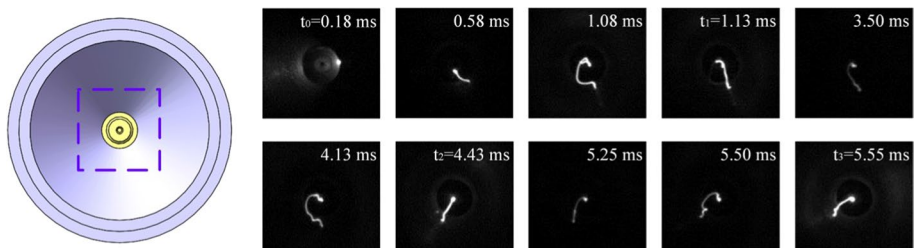
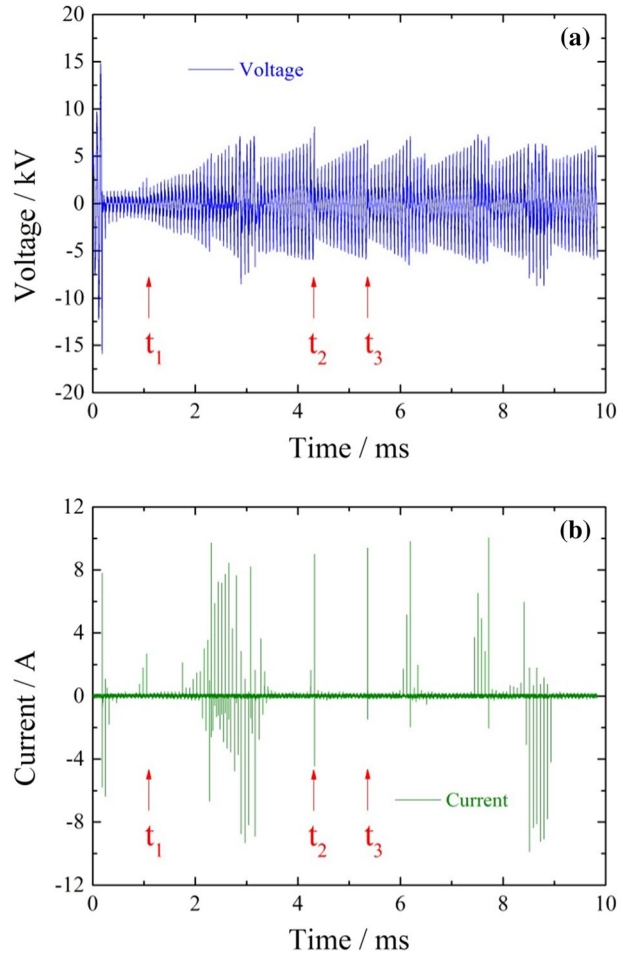


Fig. 3 Photos of gliding arc discharge by a high-speed camera at an exposure time of 23.6 μ s

Fig. 4 Details of **a** voltage and **b** current profiles of gliding arc discharge at an air flow rate of 25 L/Min



discharge [30]. The process of arc short circuit at time t_1 can be clearly seen from Fig. 3. It is worth noting that the current maintains a stable value throughout the process, except for the transition point from glow to arc, which means that the extension of the gliding arc causes the plasma resistance to increase, requiring a larger voltage. When the arc is wrinkled to cause a short circuit, the resistance decreases instantly, causing the current to peak at this moment. Then the voltage required to maintain the arc suddenly decreases. Such phenomena also occur at t_2 and t_3 . Obviously, the sudden change of the voltage waveform corresponds to the peak current, and the arc is short-circuited. This behavior of the rotating gliding arc reappears with the circumferential rotation of the arc.

As the flow rate of the medium gas increases, the gas flow becomes more turbulent, making the gliding arc more wrinkled, and the bending deformation is more serious, shortening the time from breakdown to extinction. The growth of the arc causes an increase in the voltage required to maintain the arc. However, for plasma cracking, the specific input energy is required to measure the input energy per unit fuel flow. The results show that as the gas flow increases, the energy input per unit volume decreases, which will have a negative impact on fuel cracking. In addition, the turbulent gas flow enhances the heat and

Fig. 5 The variations of specific input energy with variable flow rate

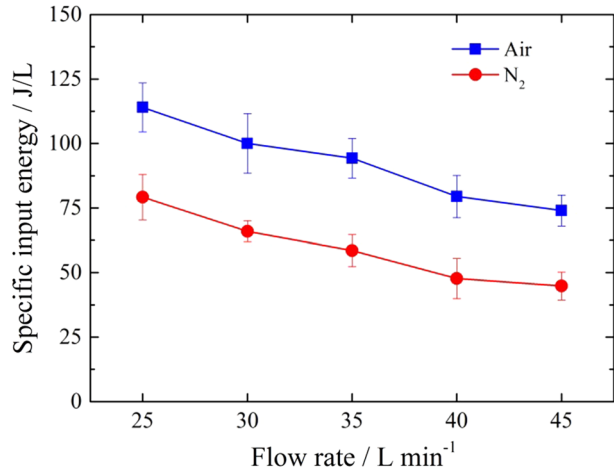
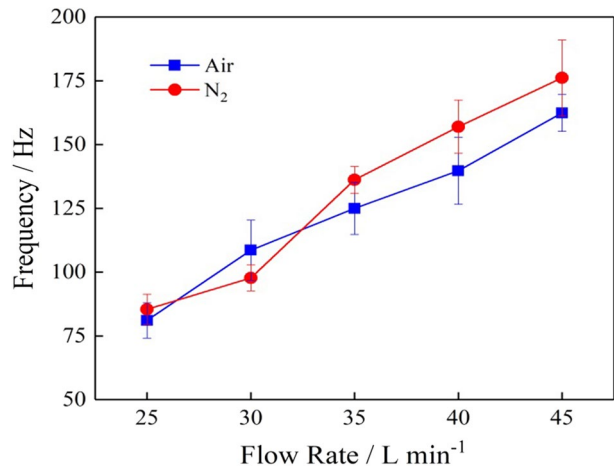


Fig. 6 The effect of flow rate on gliding arc rotational frequency



mass transfer between the thermal plasma column and the gas environment, so that the fuel cracking is at a higher temperature environment, which is an advantageous factor for fuel cracking. The gas medium uses nitrogen and air. Within the flow range of 25–45 L/min, the specific input energy and air flow rate are basically linearly correlated, as shown in Fig. 5, and when using air as the gas medium, the specific energy is greater.

Effect of Flow Rate on the Rotating Characteristics of Gliding Arc

The gliding arc rotates evenly in the venturi nozzle, which can more fully crack the fuel delivered by the fuel injector. Figure 6 counts the arc rotation frequency. The results show that the gas flow has a significant effect on the rotation frequency of the gliding arc in the entire experimental range. It is obvious that the greater the gas flow, the higher the rotation frequency. When air and nitrogen are used as the discharge medium,

the gliding arc rotation frequency is close, indicating that the arc rotation frequency is not sensitive to the gas medium. After the air flow is increased from 25 L/min to 45 L/min, the rotation frequency is doubled from 81 to 162 Hz. After the nitrogen flow rate is increased from 25 L/min to 45 L/min, the rotation frequency is increased from 85 to 176 Hz, which is also doubled. When comparing the two kinds of gas medium, the difference of rotation frequency at 40 L/min is the largest, about 20%.

It was observed in the experiment that the gliding arc discharge area was only distributed at half the height of the venturi nozzle with a volume of about 4 cm³. Combined with the gliding arc rotation frequency, at an air flow rate of 25 L/min, the treatable flow rate of plasma is 324 cm³/s, or 19.4 L/min, 77.6% of the air flow rate. This value can be used as the efficiency of the plasma sweeping gas medium. Similarly, when the air flow rate is 30 L/min, 35 L/min, 40 L/min and 45 L/min, the corresponding sweep efficiencies are 86.9%, 85.7%, 83.8% and 86.6%, respectively. When the gas medium uses nitrogen, the sweep efficiency corresponding to the flow rate from small to large is: 82.0%, 78.2%, 93.4%, 94.2%, and 93.9%. It is found that the gliding arc has higher sweep efficiency when the discharge medium is nitrogen. In fact, at every moment, the plasma arc is just a filamentary discharge channel, which does not completely fill the arc distribution area. Therefore, the above sweep efficiency index is only used as an objective reference to the relationship between the arc rotation frequency and the gas flow rate.

The distribution of rotating gliding arc is visualized, as shown in Fig. 7. Perform the short-time fourier transform on the same pixel for all photos stored under each experimental condition, to obtain the intensity value corresponding to the rotating frequency, and finally make a rotating gliding arc distribution cloud. It can be seen from the figure that the overall luminous intensity of nitrogen gliding arc discharge is stronger, which is due to the higher concentration of electronegative gas and the increase of the required loading voltage, resulting in the increase of the average discharge current. When air is selected as the discharge medium, the arc distribution is more uniform. When nitrogen is chosen as the discharge medium, the contact point between the arc and the cathode is unevenly distributed in the circumferential direction. The arc strength distribution in the annular area between the anode and the cathode is in a discrete state, which does not disperse into one piece, indicating that the distribution of the arc in the swept area is extremely unevenly distributed during the arc rotation process. This is related to the location of the arc breakdown and the corresponding short-circuit position. From the analysis in the previous section, it can be concluded that a large current will be

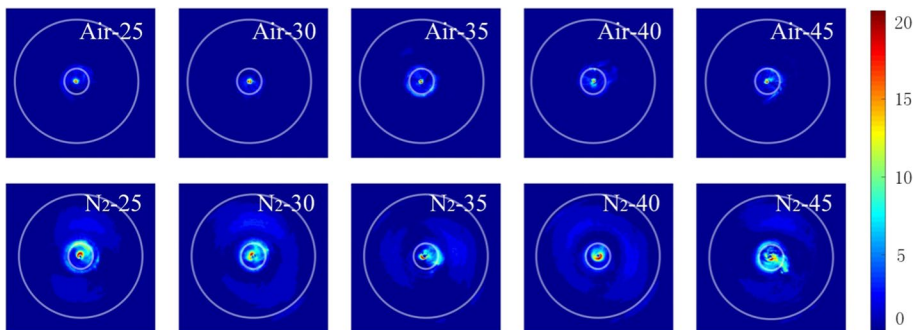


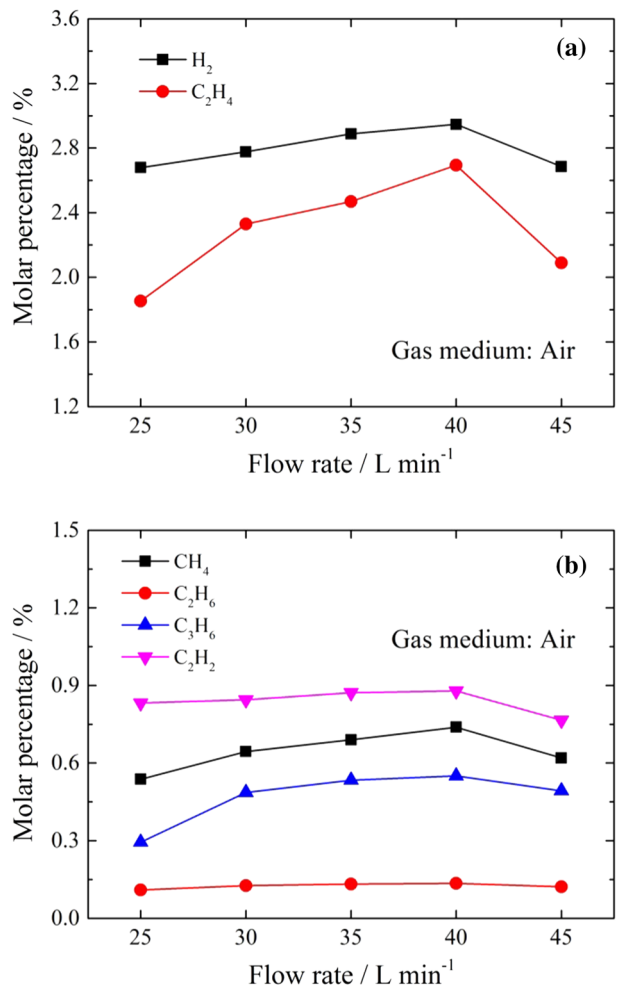
Fig. 7 Distribution uniformity of gliding arc under different experimental conditions

generated at the moment of the arc short-circuit, and the corresponding luminous intensity will be greater at this time.

Composition Distribution of Cracking Products

Gas flow is critical to the cracking product distribution. Figure 8 shows the change of product concentration with flow rate under the discharge medium of air. The concentration order of product from high to low is hydrogen, ethylene, acetylene, methane, propylene, and ethane, ignoring the components whose concentration is in the order of 1/10,000. In addition, the gas sample contains an average of about 7.8% oxygen and 2.7% carbon dioxide, and the rest is nitrogen. It can be seen from the figure that with the increase of the air flow rate, the concentration of each component increases first and then decreases. At a flow rate of 40 L/min, the concentration of each component is the largest, and the hydrogen concentration reaches a maximum of 2.9%. Although the specific input energy tends to

Fig. 8 Molar percentage of **a** H_2 and C_2H_4 , **b** CH_4 , C_2H_6 , C_3H_6 and C_2H_2 in the cracking gas with various air flow rate



decrease as the flow rate increases, it can be seen from the change trend of the component concentration in Fig. 8 that before 40 L/min, as the flow rate increases, the energy utilization rate increases. As the second highest concentration species, ethylene is most affected by the change of flow rate. During the increase of air flow from 25 L/min to 40 L/min, the ethylene concentration increased from 1.8% to 2.7%, which increases by 33%. While the air flow increased from 40 L/min to 45 L/min, the ethylene concentration in the product quickly dropped to 2.1%, which drops by 22%. Since ethylene contains more hydrogen elements, the wide fluctuations range of ethylene concentration will play a leading role in the change of hydrogen selectivity in the product. Acetylene, as the active species with the smallest detonation cell size and the lowest critical initiation energy, accounts for nearly 1% of the cracking gas. This content is very considerable for increasing the initiation probability.

After changing the gas medium to nitrogen, the content of active components in the gaseous product was significantly reduced. Species with concentrations above 1/10,000 include hydrogen, ethylene and acetylene, and the concentrations of the three components are all below 0.5%. The component with the highest concentration is still hydrogen. This is because the $C_{\beta}-C_{\gamma}$ bond in the n-decane molecule is the weakest. In the process of plasma cracking n-decane, the high energy particles and n-decane collide with each other to break the $C_{\beta}-C_{\gamma}$ bond, and the ethyl and octyl groups are most easily generated. The ethyl group then undergoes $C_{\beta}-H$ bond breaking to produce ethylene, and the formed hydrogen atoms act as free radicals to attack other alkyl groups to undergo dehydrogenation to generate hydrogen. The chain reaction is initiated, generating more free radicals and hydrogen atoms. Therefore, the content of hydrogen and ethylene in the cracking products is usually higher. However, it was found in this experiment that the content of ethylene is even lower than that of acetylene when nitrogen is used as the gas medium. The possible reason is that the production of acetylene and ethylene requires the consumption of ethyl groups, and the reaction path for the formation of acetylene in a nitrogen plasma environment is more competitive. As the nitrogen flow rate increases, the acetylene content decreases, while the ethylene content increases, indicating that the advantage of acetylene production gradually decreases. The hydrogen concentration decreases with increasing nitrogen flow rate, which is mainly due to the decrease in specific energy input.

Hydrogen selectivity refers to the proportion of hydrogen atoms contained in hydrogen in all hydrogen atoms contained in the gaseous product formed by cracking n-decane. Hydrogen is the species with the highest calorific value among all fossil fuels, reaching 1.4×10^8 J/kg, and it is highly flammable and easy to knock. Adding a small amount of hydrogen to the detonation engine plays an important role in improving the detonation performance. Therefore, hydrogen selectivity is an important indicator to measure the cracking effect. Figure 10 reveals the change of hydrogen selectivity with flow rate when air and nitrogen are gaseous medium. When the nitrogen plasma cracks n-decane, the average hydrogen selectivity is higher. The change of hydrogen selectivity shows the opposite trend when using two different gas medium. When using nitrogen, the hydrogen selectivity decreases slowly and then decreases sharply, while the selectivity decreases first and then increases sharply under the medium of air. The main reason for this phenomenon is that under the experimental conditions of this paper, the ethylene content in the cracking gas is higher, and ethylene is a species with more hydrogen elements, and its concentration has a great influence on the trend of hydrogen selectivity. Combined with Figs. 8 and 9, when the flow rate increases from 40 L/min to 45 L/min, the ethylene concentration in the product decreases sharply when air plasma is used, while the ethylene concentration in the product increases significantly when nitrogen plasma is used. Eventually, the hydrogen selectivity

Fig. 9 Molar percentage of H_2 , C_2H_4 and C_2H_2 in the cracking gas with various nitrogen flow rate

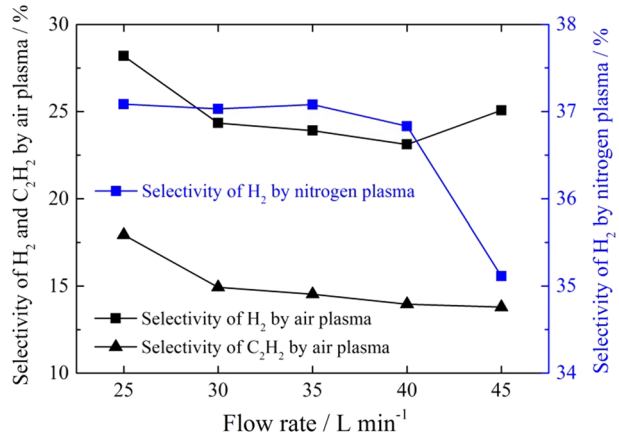
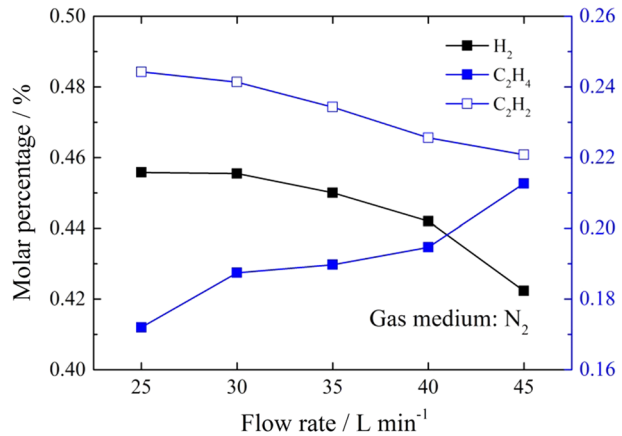


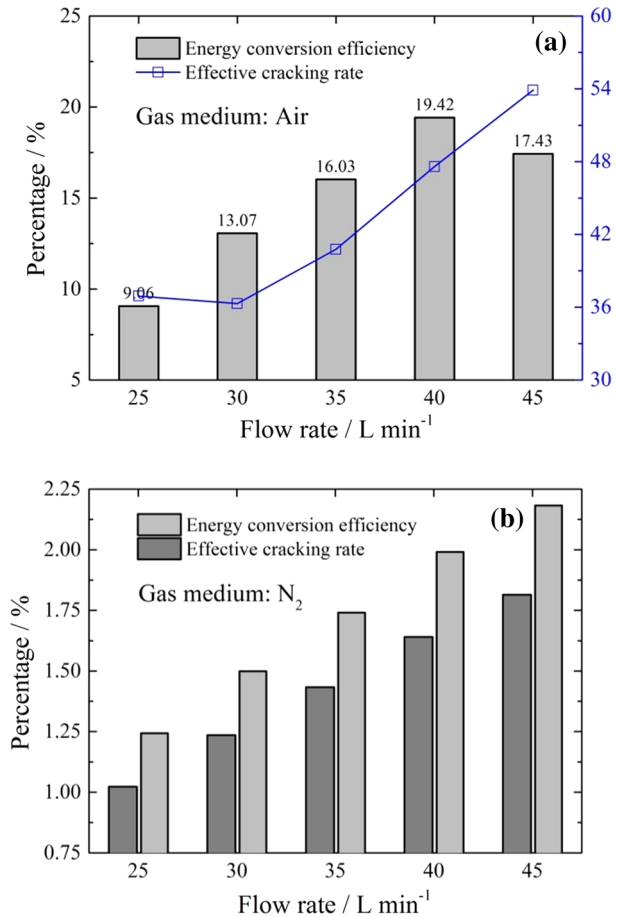
Fig. 10 Hydrogen and acetylene selectivity with various flow rate under nitrogen and air as discharge medium



will show the opposite trend under the corresponding working conditions. As a component with the smallest detonation cell size, acetylene selectivity is in the range of 13%–18%. With the increase of air flow rate, the selectivity of acetylene decreases gradually. It shows the weakening of the plasma treatment ability at high flow rate.

The energy conversion efficiency and carbon based characterization effective cracking rate are used to measure the cracking effect. The energy conversion efficiency is obtained by dividing the total low heating value of all components in the cracking product by the low heating value of the n-decane supplied (Eq. 4). The effective cracking rate is the ratio of the mass of carbon atoms in the cracking product to the total carbon amount in n-decane supplied (Eq. 5). As shown in Fig. 11a, the two indexes change with flow rate under the condition of air plasma. The energy conversion efficiency and product concentration showed a consistent trend, reaching a maximum value of 19.42% at a flow rate of 40 L/min, indicating that the index of energy conversion efficiency is positively correlated with the total content of cracking products. The change trend of the effective cracking rate is different. It gradually increases with the increase of the flow rate, and reaches the maximum value of 53.9% when the air flow rate is 45 L/min. This

Fig. 11 Energy conversion efficiency and carbon-based characterization effective cracking rate varies with flow rate under **a** air and **b** nitrogen as discharge medium



is mainly because the carbon dioxide contained in the cracking gas is taken into account when calculating the effective cracking rate. After all, the carbon element in carbon dioxide is derived from n-decane fuel. As the air flow rate increases, the proportion of n-decane participating in the oxidation gradually increases, and the carbon dioxide content in the cracking gas also increases. Because the carbon dioxide concentration is higher than the ethylene concentration, it contributes a lot to the effective cracking rate, making this indicator always show an upward trend. In summary, for the air plasma cracking of n-decane, it is more reliable to use the index of energy conversion efficiency to evaluate the cracking effect and the content of active components in the cracking gas.

For the nitrogen plasma, both the energy conversion efficiency and the effective cracking rate increase with the increase of the nitrogen flow rate, but both remain at a low level. When the nitrogen flow rate is 45 L/min, the two indicators are 2.2% and 1.8% respectively. It is worth noting that the concentration of components other than ethylene in the cracking product decreases with increasing flow rate, but the actual yield has not decreased. For example, the hydrogen output is 0.11 L/min at a nitrogen flow rate of 25 L/min, and 0.19 L/min at a nitrogen flow rate of 45 L/min. In addition, the supply flow of n-decane is the same under all operating conditions, which ultimately

leads to an increase in the energy conversion efficiency and effective cracking rate as the nitrogen flow rate increases.

Conclusions

The experiment of n-decane cracking with plasma was carried out in a new type of gliding arc flow reactor. Nitrogen and air were used as gas medium in the experiment. The evolution process and the discharge characteristics of the gliding arc under different flow rate were compared. It is found that the larger the gas flow rate is, the higher the rotating frequency of the gliding arc is, and there is no direct relationship with the type of gas. The electronegativity of oxygen is higher than that of nitrogen, which leads to a higher arc strength and a more uneven arc distribution. Although nitrogen as gas medium has a higher sweep efficiency than air gliding arc, air plasma has a higher specific input energy.

The cracking characteristics and efficiency under different gas types and gas flow rates were studied. When air is discharge gas, the cracking products include hydrogen, ethylene, acetylene, methane, propylene and ethane. At a flow rate of 40 L/min, the concentration of each component is the largest, with the hydrogen concentration reaching a maximum of 2.9%. After changing the discharge gas to nitrogen, the main cracking products include hydrogen, ethylene and acetylene, and the content of active components in the gaseous product is significantly reduced. Due to the influence of ethylene content, the hydrogen selectivity shows the opposite law when choosing different gas types. In nitrogen, the hydrogen selectivity first decreases slowly and then decreases sharply, while in air, the selectivity first decreases and then increases sharply.

The cracking effect of the flow reactor is measured by introducing energy conversion efficiency and carbon-based characterization effective cracking rate. The energy conversion efficiency and product concentration show a consistent pattern with using air plasma, but the change trend of the effective cracking rate is different. This is mainly because the carbon dioxide contained in the cracked gas is taken into account when calculating the effective cracking rate. For nitrogen plasma, both the energy conversion efficiency and the effective cracking rate increase with increasing nitrogen flow, but both remain at a low level. Therefore, it is more reliable to use the index of energy conversion efficiency to evaluate the cracking effect and the content of active components in the cracked gas.

Acknowledgements Research reported in this publication was supported by the National Natural Science Foundation of China (Grant Nos. 91941105, 91941301, 51790511).

References

1. Kaemming TA, Fotia M, Hoke J et al (2017) Thermodynamic modeling of a rotating detonation engine through a reduced-order approach. *J Propuls Power* 33(5):1170–1178
2. Frolov SM, Aksenov VS, Ivanov VS (2015) Experimental proof of Zel'dovich cycle efficiency gain over cycle with constant pressure combustion for hydrogen–oxygen fuel mixture. *Int J Hydrog Energy* 40(21):6970–6975
3. Andrews G et al. (2018) Preliminary Design of a Rotating Detonation Engine for Launch Vehicle Applications. 2018 AIAA Aerospace Sciences Meeting
4. Huff R et al. (2019) Exit Condition Measurements of a Radial Rotating Detonation Engine Bleed Air Turbine. AIAA Scitech 2019 Forum
5. Frolov SM, Ivanov VS, Shamshin IO et al (2019) Kerosene-fueled turbojet afterburner operating on detonative combustion. In: 10th international workshop on detonation for propulsion, pp. 44–47. <https://doi.org/10.30826/IWDP201916>, <http://www.frolovs.ru/pdf/2019-25-eng.pdf>

6. Bykovskii FA, Zhdan SA, Vedernikov EF (2006) Continuous spin detonation of fuel-air mixtures. *Combust Explos Shock Waves* 42(4):463–471
7. Liu S, Peng H, Liu W et al (2020) Effects of cavity depth on the ethylene-air Continuous Rotating Detonation. *Acta Astronaut* 166:1–10
8. Dincer I, Acar C (2016) A review on potential use of hydrogen in aviation applications. *Int J Sustain Aviat* 2(1):74–100
9. Kindracki J (2015) Experimental research on rotating detonation in liquid fuel–gaseous air mixtures. *Aerosp Sci Technol* 43(43):445–453
10. Zhong Y et al (2019) Investigation of rotating detonation fueled by the pre-combustion cracked kerosene. *Aerosp Sci Technol* 95:105480
11. Wolański P, Kalina P, Balicki W et al (2018) Development of gasturbine with detonation chamber//detonation control for propulsion. Springer, Cham, pp 23–37
12. Kindracki J (2015) Experimental research on rotating detonation in liquid fuel–gaseous air mixtures. *Aerosp Sci Technol* 43:445–453
13. Brabbs, TA (1993) Fuel-rich catalytic combustion of a high density fuel. Vol. 3281. National Aeronautics and Space Administration, Office of Management, Scientific and Technical Information Program
14. Austin JM, Shepherd JE (2003) Detonations in hydrocarbon fuel blends. *Combust Flame* 132(1–2):73–90
15. Wierzbicki TA, Lee IC, Gupta AK (2016) Recent advances in catalytic oxidation and reformation of jet fuels. *Appl Energy* 165:904–918
16. Wang Q, Yan BH, Jin Y et al (2009) Investigation of dry reforming of methane in a dielectric barrier discharge reactor. *Plasma Chem Plasma Process* 29(3):217–228
17. Barni R, Benocci R, Spinicchia N et al (2019) An experimental study of plasma cracking of methane using DBDs aimed at hydrogen production. *Plasma Chem Plasma Process* 39(1):241–258
18. Khosravi A, Khani MR, Goy ED et al (2018) The processing of pyrolysis fuel oil by dielectric barrier discharge plasma torch. *Plasma Chem Plasma Process* 38(2):365–378
19. Khani MR, Khosravi A, Dezhbangooy E et al (2014) Study on the feasibility of plasma (DBD reactor) cracking of different hydrocarbons (n-hexadecane, lubricating oil, and heavy oil). *IEEE Trans Plasma Sci* 42(9):2213–2220
20. Rueangjitt N, Sreethawong T, Chavadej S et al (2011) Non-oxidative reforming of methane in a mini-gliding arc discharge reactor: effects of feed methane concentration, feed flow rate, electrode gap distance, residence time, and catalyst distance. *Plasma Chem Plasma Process* 31(4):517–534
21. Jiang N, Qiu C, Guo L et al (2019) Improved performance for toluene abatement in a continuous-flow pulsed sliding discharge reactor based on three-electrode configuration. *Plasma Chem Plasma Process* 39(1):227–240
22. Sreethawong T, Thakonpatthanakun P, Chavadej S (2007) Partial oxidation of methane with air for synthesis gas production in a multistage gliding arc discharge system. *Int J Hydrog Energy* 32(8):1067–1079
23. Rollier JD, Gonzalez-Aguilar J, Petitpas G et al (2007) Experimental study on gasoline reforming assisted by nonthermal arc discharge. *Energy Fuels* 22(1):556–560
24. Paulmier T, Fulcheri L (2005) Use of non-thermal plasma for hydrocarbon reforming. *Chem Eng J* 106(1):59–71
25. Taghvaei H, Jahanmiri A, Rahimpour MR et al (2013) Hydrogen production through plasma cracking of hydrocarbons: effect of carrier gas and hydrocarbon type. *Chem Eng J* 226:384–392
26. Song F, Wu Y, Xu S et al (2019) N-decane decomposition by microsecond pulsed DBD plasma in a flow reactor. *Int J Hydrog Energy* 44(7):3569–3579
27. Song F, Jin D, Jia M et al (2017) Experimental study of n-decane decomposition with microsecond pulsed discharge plasma. *Plasma Sci Technol* 19(12):125502
28. Song F, Jin D, Wu J et al (2019) Experimental investigation on the plasma decomposition of n-decane under the atmospheric pressure argon environment. *High Volt Eng* 45(2):618–623
29. Xu S, Jin D, Song F et al (2019) Experimental investigation on n-decane plasma cracking in an atmospheric-pressure argon environment. *Plasma Sci Technol* 21(8):085503
30. Gangoli SP (2007) Experimental and modeling study of warm plasmas and their applications. ProQuest